

Incorporation CdS with ZnS as nanocomposite and Using in Photo-Decolorization of Congo Red Dye

Faten Hadi Fakhri and Luma Majeed Ahmed*

Department of Chemistry, College of Science, University of Kerbala, Kerbala 56001, Iraq

* Corresponding author:

email: lumamajeed2013@gmail.com

Received: August 27, 2018

Accepted: October 9, 2018

DOI: 10.22146/ijc.38335

Abstract: The aim of this manuscript was to modify the ZnS surface by incorporating with CdS photocatalyst. This manner led to depressing the recombination process and increasing the activity. The X-ray Powder Diffraction (XRD) data were proved that the CdS incorporated with ZnS and formed ZnS-CdS nanocomposite by observing new peaks at 26.92°, 28.62°, 30.52°, and 47.26°. Based on the Atomic Force Microscopy (AFM) analysis and Tauc equation, the particle sizes for all samples were raised with decreased the band gap values. The activation energy for decolorization of Congo red with the using ZnS is found to be more than that value for the using prepared ZnS-CdS nanocomposite. The percentage of efficiency was found to be increased with modified the ZnS surface.

Keywords: Congo red dye; ZnS; ZnS-CdS nanocomposite; photo-decolorization

■ INTRODUCTION

In the few last decades, the raised of utilized from the photocatalysts and nanocatalysts was regarded as versatile materials such as produced of solar cells [1-2], decolorized and degradation of organic compounds [3-8] used as biosensor [9-10], synthesis some organic compounds in certain reactions [11], using as anticancer and antitumor [12-13], and using in SPF solar emulsions as sunscreen [14-15].

Today, ZnS is deemed one of the best II-VI photoactive semiconductors that used to manufacture the solar cells [16-18]. It is being non-toxic, high refractive index, high abundant, eco-friendly of an environment, non-cost and having a good chemical stability. Moreover, ZnS is existence in two crystalline forms: cubic ZnS form and hexagonal ZnS form [19-21], it also has two direct wide band gap energy approximately equal to 3.54 and 3.91 eV for zinc blend (cubic ZnS form) and wurtzite (hexagonal ZnS form) respectively [22]. Both values of ZnS band gaps are large and will raise the recombination process. In order to abate this problem, some researchers had been published many numbers of manuscripts in this field. Mahammed and Ahmed modified the surface of ZnS by doped Cr [23] and the doped mixture from Cr and Mn [24] on his surface with using co-precipitation

method to improve the optical properties and using them in decolorization of reactive black 5 dye.

CdS are related to II-VI photoactive semiconductor group too and have a small band gap (2.4 eV) at 300 K. That rehabilitated it to use as the photocatalyst in solar cells, in photocatalysis, in the manufacturing of Light-emitting diodes (LEDs) and transistors, and treatment of wastewater [25-26]. Hence, some researchers interested with the incorporation of CdS with ZnS crystal lattice to increase the efficiency of photoreaction of ZnS. Fang and coworkers [27] employed the simple chemical precipitation process via decorated ZnS core with tiny CdS and produced ZnS-CdS nanocomposite. This nanocomposite was used to investigate the photocatalytic efficiency towards Rhodamine B and found it is about three times as much as that of pure ZnS cores. Raubach and co-workers [28] prepared CdS@ZnS core-shell system by using the microwave- assisted solvothermal technique, then studied the structural and optical approach CdS, ZnS and CdS@ZnS core-shell compound.

The goal of this manuscript was included the modification of ZnS surface by incorporating the CdS and produced ZnS-CdS nanocomposite. The XRD analysis, AFM analysis, and Tauc equation were done, and then the compared the photoactivity of ZnS and

ZnS-CdS nanocomposite in decolorization of Congo red dye in aqueous solution was determined.

EXPERIMENTAL SECTION

Materials

All the employed chemical materials were used without any subsequent treatments. 99.5% purity of ZnS, CdCl₂·2H₂O, and thiourea were purchased from Fluka. Congo red (direct red 28) dye was supplied by Merck. This dye is having a chemical class type diazo, the molecular formula is C₃₂H₂₂N₆Na₂O₆S₂, IUPAC name is sodium salt of 3,3'-([1,1'-biphenyl]-4,4'-diyl)bis(4-aminonaphthalene-1-sulfonic acid), M.Wt is 696.665 g/mol, λ_{max} is 497–500 nm, and the chemical structure explains in Fig. 1.

Instrumentation

X-Ray Diffraction Spectroscopy (Lab X- XRD 6000) and UV- Visible spectrophotometer (AA-1800) were supplied from Shimadzu, Japan. The initial pH of dye solution was conducted by employing a pH meter (type WTW Inolab pH720 - Germany). Particle sizes for all samples were carried out using AFM (AA 3000, Advanced Angstrom Inc., USA). The common instruments that employed in this manuscript were have consisted on the centrifuge (Hettich- Universal II- Germany), sensitive balance (BL 210 S, Sartorius, Germany), magnetic stirrer (Heido-MrHei-Standard, Germany) and Ultrasonic (DAIHAN Scientific, Korea). A photoreactor equipped with the ultraviolet lamp (HPML, 400 W, Radium, China) was employed as a photo-decolorization chamber, as depicted in Fig. 2.

Procedure

Preparation of ZnS-CdS nanocomposite

ZnS-CdS nanocomposite was prepared by using a modified method as mentioned in reference [29], this method was done under reflex reaction at 80 °C for 9 h. Exactly, 2 mmoles (0.163 g) of zinc sulfide were dispersed in ethanol under ultrasonic to get homogeneous ZnS solution as (solution 1), then 1 mmole (0.219 g) of cadmium chloride dihydrate and 1 mmole (0.152 g) of

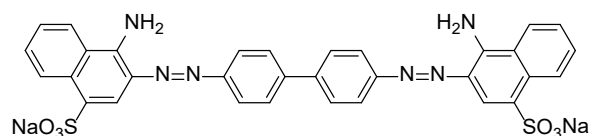


Fig 1. Chemical structure of Congo red dye

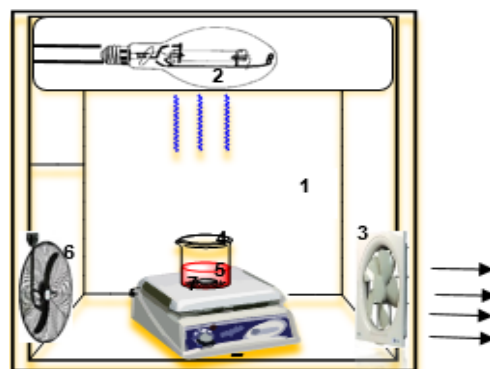


Fig 2. Schematic diagram of experimental set-up (photocatalytic reactor unit), consisted of: (1) wooden box, (2) mercury lamp type high pressure (400 W), (3) vacuum fan, (4) pyrex glass beaker size 400 cm³, (5) teflon bar, (6) fan and (7) magnetic stirrer

thiourea were dissolved in ethanol and D.W under ultrasonic as a (solution 2) and as a (solution 3), respectively.

Solution 2 is used as a Cd precursor, which was dropwise added into ZnS suspension solution (solution 1) and formed a mixture. The solution 3 of thiourea is regarded as a sulfur precursor that was added drop by drop into the last mixture and produced a white mixture. This white mixture was turned to a light yellow color with stirred and heated by reflux process at 80 °C for 9 h, to ensure the reaction was fully completed. This light yellow color mixture was filtrated and washed by ethanol, then saved overnight at room temperature in desecrator.

Photocatalytic activity for ZnS and ZnS-CdS nanocomposite

The photocatalytic activity of the ZnS and ZnS-CdS nanocomposite catalysts was investigated by decolorization of Congo red dye under UV-A light, which has a light intensity equal to 3.189×10^{-7} Enstine S⁻¹. 100 mL from 50 ppm of Congo red dye solution was

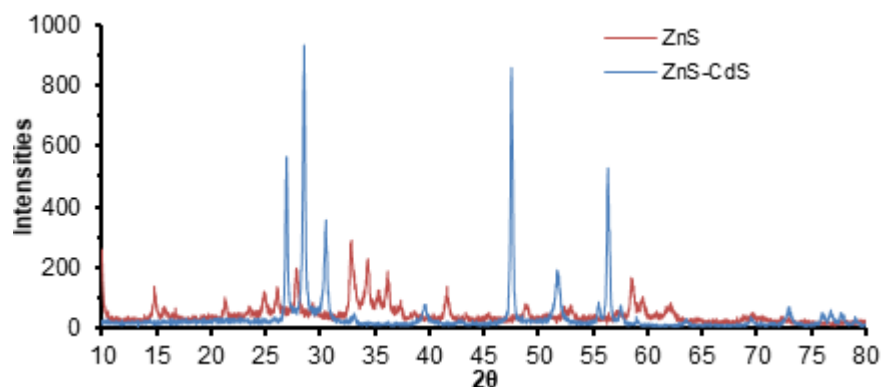


Fig 3. The XRD patterns of ZnS and ZnS-CdS nanocomposite

prepared in cold D.W and then mixed with 0.1 g from ZnS and 0.1 g from prepared ZnS-CdS nanocomposite. The reaction mixtures were carried out at an initial pH equal to 7.0 and temperatures ranged from 10 °C to 30 °C. Firstly, the dark reaction was performed for these mixtures with continuous stirring for 30 min, and then the light was focused on these suspension solutions in intervals time. Approximately 3 mL from mixtures were collected and double carefully centrifuged.

The absorbance of the filtered dye solutions was measured at 500 nm. By basing on the calibration curve of dye, the residue concentration of dye was found. At the low concentration of studied dye, the Langmuir-Hinshelwood kinetic expression was utilized to determine the rate constant (k_{app}) for this photoreaction and the efficiency of photodecolorization percentage (E %), as expressed by the following equations [30-31].

$$\ln\left(\frac{C_o}{C_t}\right) = k_{app} \cdot t \quad (1)$$

$$E \% = \left(\frac{C_o - C_t}{C_o}\right) \times 100 \quad (2)$$

where C_o is an initial concentration of Congo red dye without irradiation. C_t is a concentration of the same dye at the time t of irradiation.

RESULTS AND DISCUSSION

Structural Property

XRD analysis was used to identify the structure and phase for powder ZnS and prepared ZnS-CdS nanocomposite, as presented in Fig. 3. The sharp peaks in the blue line indicated to the prepared ZnS-CdS

nanocomposite is more crystal from the used ZnS as a precursor. Practically, the XRD patterns for ZnS show four diffraction peaks, the first is a strong peak at $2\theta = 27.08^\circ$ which belong to (111) reflection of the cubic zinc blende structure of ZnS (JCPDS No 5-566) [32-34]. But the weak peaks have occurred at $2\theta = 32.78^\circ$, 48.68° , and 58.44° which assigned to (200), (220), (311) [34-35]. The three clear peaks of hexagonal CdS in blue line are observed at 26.92° , 28.62° , and 30.52° correspond to (002), (101) and (200) planes, (JCPDS-89-2944) respectively [36]. On the other hand, one relative sharp peak at 47.26° which corresponding to (220) plane (JCPDS Card No.-75-1546) [26,37]. The prominent weak peak are observed at 51.36° which corresponding to (311) and (103) plane as cubic CdS [27,38] (JCPDS Card No. 75-1546) and (JCPDS 01-080-0006), hexagonal CdS is had somewhat weaker peak at 39.36° in (102) plane this agreement with reference [39]. Some peaks such as 48.66° , 58.5° , and 52.3° of ZnS are shifted to a lower angle (2θ), this behavior is confirmed that the metal bond is formed [23], so, Cd is incorporated with Zn lattice and produced ZnS-CdS as a nanocomposite.

Surface Morphology

Atomic force microscopy (AFM) images were recorded in Fig. 4 and 5, it is observed that the particle size of ZnS is smaller than that value for ZnS-CdS nanocomposite and equal to 77.60 and 80.05 nm, respectively. This is attributed to the low ionic radius for Zn (0.75 \AA) compared with the ionic radius of Cd (0.95 \AA) [40]. Moreover, the ZnS-CdS nanocomposite has more agglomeration than ZnS sample.

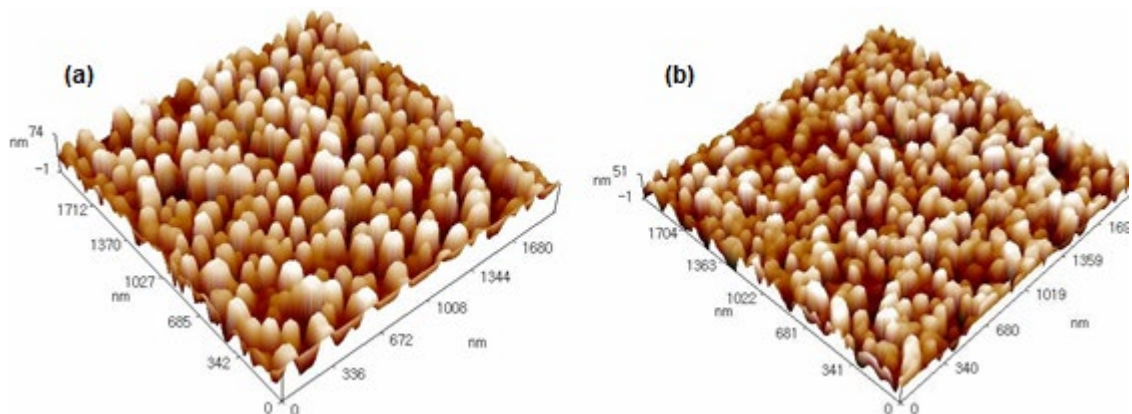


Fig 4. The AFM three dimension images (a) ZnS and (b) ZnS-CdS nanocomposite

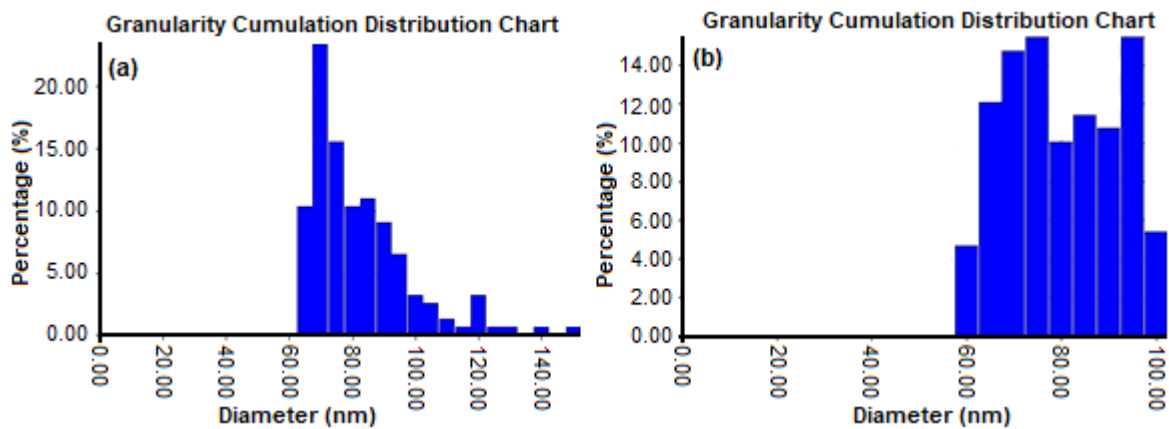


Fig 5. The Histograms of AFM analysis (a) ZnS and (b) ZnS-CdS nanocomposite

Optical Property

Tauc plots [36,41-42] were determined to explore the optical properties as the direct band gap of ZnS and ZnS-CdS nanocomposite, as mentioned in equation (3).

$$\alpha h\nu = k(h\nu - E_g)^m \quad (3)$$

where h is Plank's constant, ν is the frequency of the incident photon light and equal to (C/λ) , C is light rate and λ wavelength. k is optical constant (depended on different transition and the effective masses of electron and hole), E_g is band gap in (eV), m is a constant value which equal to $\frac{1}{2}$ for a direct transition.

Besides, α is the absorption coefficient, A is absorbance, t is path thickness, α is calculated by the following equation in reference [35].

$$\alpha = 2.3026 A / t \quad (4)$$

The exact values of the direct band gap of ZnS and ZnS-CdS nanocomposite are measured by extrapolating

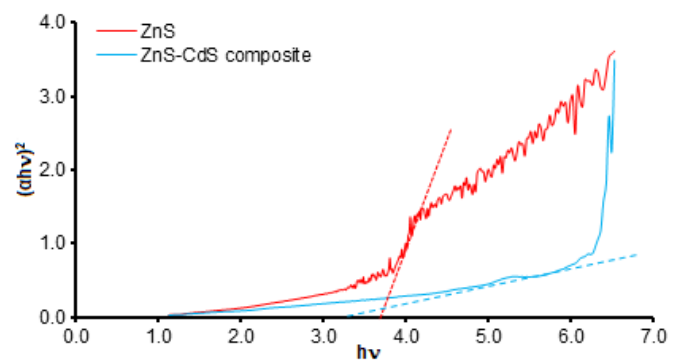


Fig 6. Tauc plot for ZnS and ZnS-CdS nanocomposite

the straight line portion of $(\alpha h\nu)^2$ versus $h\nu$. As shown in the inset of Fig. 6. The direct band gaps for ZnS and ZnS-CdS nanocomposite are equal to 3.6 and 3.1 eV, respectively. These values found that the band gap values decrease with increasing of particle size. This behavior is an agreement with the redshift that occurred in reference [43].

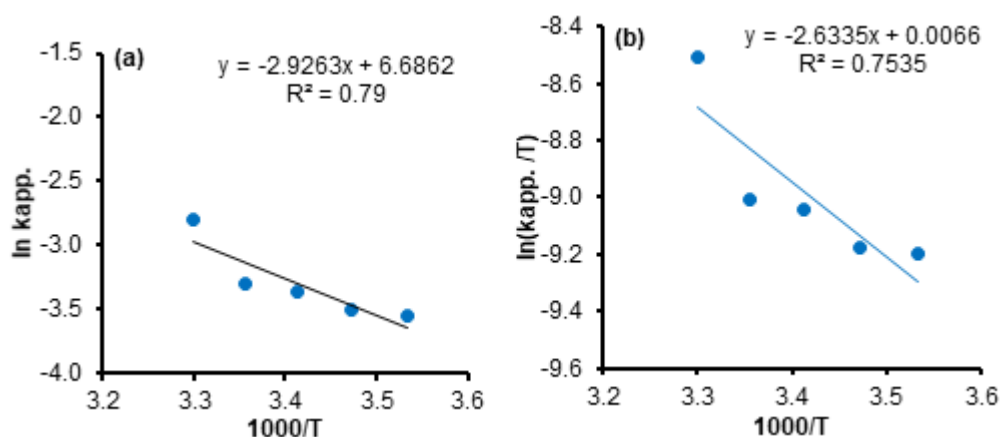


Fig 7. Effect of temperature in the range (283–303) K on the photodecolorization of Congo red dye from suspension solution of 100 mg/100 mL ZnS (a) Arrhenius equation plot and (b) Eyring plot

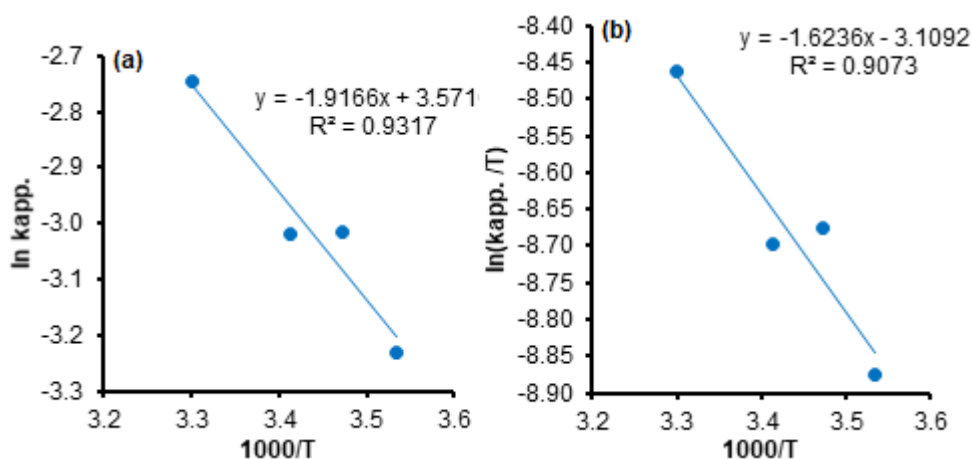


Fig 8. Effect of temperature in the range (283–303) K on the photodecolorization of Congo red dye from suspension solution of 100 mg/100 mL ZnS-CdS nanocomposite at the range temperatures (283–303) K (a) Arrhenius equation plot and (b) Eyring plot

Table 1. The activation kinetic and thermodynamic parameters for photo-decolorization of Congo red dye with the using ZnS and ZnS-CdS nanocomposite

	E_a (kJ mol ⁻¹)	ΔH^\ddagger (kJ mol ⁻¹)	ΔS^\ddagger (J mol ⁻¹ K ⁻¹)	ΔG^\ddagger_{303} (kJ mol ⁻¹)
ZnS	24.329	21.894	-2.857	22.761
ZnS-CdS nanocomposite	15.935	13.499	-3.232	14.479

Effect of Temperature on Photodecolorization of Congo Red Dye

The temperature is a vital factor to enhance the photoreaction, the effect of temperature was illustrated in ranged (10–30) °C. The activation energy and some thermodynamic parameters were found by depending on the Arrhenius equation, Eyring equation and Gibbs equation [44-45].

Based on the above results for linear relations, as indicated in Fig. 7 and 8, the activation energies and thermodynamic parameters values are tabulated in Table 1.

It was observed that the activation energies values with the using the prepared ZnS-CdS nanocomposite is less than that value for the employing ZnS as a photocatalyst, that confirmed the using of ZnS-CdS

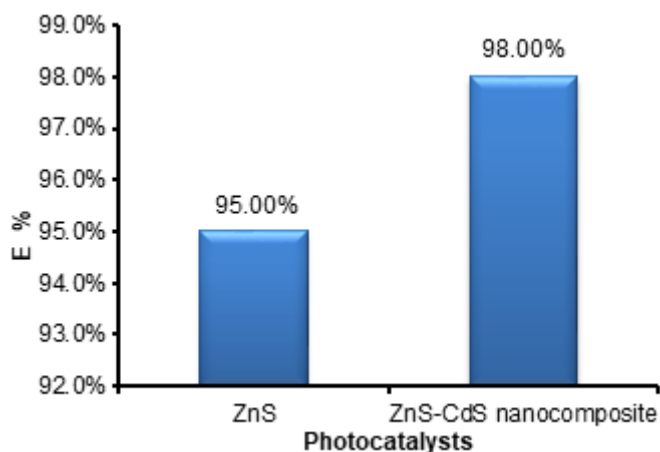


Fig 9. The relation between photodecolorization of Congo red dye efficiency and types of used photocatalysts

nanocomposite is favored because of the photoreaction the using of ZnS-CdS nanocomposite is faster than that photoreaction with used ZnS only.

Both photodecolorization of Congo red dye using ZnS and ZnS-CdS nanocomposite are endothermic, less random and non-spontaneous reactions. The positive value of ΔG^\ddagger is illustrated, that the high solvated structure obtains in a transition state between hydroxyl radicals and dye (Congo red dye) molecules. This case is in agreement with the results that reported by references [6,24,46-47].

At 30 °C and 1h from irradiation for Congo red dye in the presences ZnS and ZnS-CdS nanocomposite, the photodecolorization efficiency is elevated with using ZnS-CdS nanocomposite compared with the using ZnS alone and found to be equal 98.241 and 94.594% respectively, as depicted in Fig. 9.

■ CONCLUSION

This present work found the photodecolorization of efficiency with using ZnS-CdS nanocomposite to be more than 98% at the following optimum condition: temperature 30 °C, initial pH of Congo red dye solution is 7.0 and 100 mg of prepared ZnS-CdS nanocomposite. This behavior depended on the ability of modified ZnS surface to depress the recombination process and rise from produced of the hydroxyl radicals. Moreover, the activation energy decreases from 24.32 to 15.93 kJ mol⁻¹. XRD data and AFM image were confirmed to successfully form for ZnS-CdS nanocomposite. The band gap was

depressed with incorporated of Cd with Zn and produced ZnS-CdS nanocomposite.

■ REFERENCES

- [1] Jafarov, M.A., Nasirov, E.F., Jahangirova, S.A., and Jafarli, R., 2015, Nano-ZnS thin films for solar cell, *Nanosystems: Phys. Chem. Math.*, 6 (5), 644–649.
- [2] You, R.W., and Fu, Y.P., 2016, Zinc sulfide buffer layer for CIGS solar cells prepared by chemical bath deposition, *Adv. Technol. Innovation*, 2 (3), 95–98.
- [3] Muslim, Z.R., and Kadhim, R.F., 2017, Photocatalytic removal of methylene blue dye by using of ZnS and CdS, *Iraq. J. Phys.*, 15 (33), 11–16.
- [4] Kaur, S., 2017, A brief review on photocatalytic activity of ZnS and CQDs nanoparticles, *Int. J. Eng. Appl. Sci. Technol.*, 2 (4), 75–82.
- [5] Purnawan, C., Wahyuningsih, S., and Kusuma, P.P., 2016, Photocatalytic and photoelectrocatalytic degradation of methyl orange using graphite/PbTiO₃ nanocomposite, *Indones. J. Chem.*, 16 (3), 347–352.
- [6] Ahmed, L.M., Saeed, S.I., and Marhoon, A.A., 2018, Effect of oxidation agents on photo-decolorization of vitamin B₁₂ in the presence of ZnO/UV-A system, *Indones. J. Chem.*, 18 (2), 272–278.
- [7] Usman, M.R., Noviyanti, A.R., and Eddy, D.R., 2017, Photocatalytic degradation of diazinon using titanium oxide synthesized by alkaline solvent, *Indones. J. Chem.*, 17 (1), 22–29.
- [8] Yuliati, L., Roslan, N.A., Siah, W.R., and Lintang, H.O., 2017, Cobalt oxide-modified titanium dioxide nanoparticle photocatalyst for degradation of 2,4-dichlorophenoxyacetic acid, *Indones. J. Chem.*, 17 (2), 284–290.
- [9] Singh, P., Abdullah, M.M., and Ikram, S., 2016, Role of nanomaterials and their applications as photocatalyst and sensors: A review, *Nano Res. Appl.*, 2 (1), 1–10.
- [10] Erdiven, U., Karaaslan, M., Unal, E., and Karadağ, F., 2012, Planar photonic crystals biosensor applications of TiO₂, *Acta Phys. Pol. A*, 122 (4), 732–736.
- [11] Fatimah, I., Rubiyanto, D., and Kartika, N.C., 2016, Effect of calcination temperature on the synthesis of ZrO₂-pillared saponite to catalytic activity in

- menthol esterification, *Indones. J. Chem.*, 16 (1), 8–13.
- [12] Kalbacova, M., Macak, J.M., Schmidt-Stein, F., Mierke, C.T., and Schmuki, P., 2008, TiO₂ nanotubes: Photocatalyst for cancer cell killing, *Phys. Status Solidi RRL*, 2 (4), 194–196.
- [13] Vinardell, M.P., and Mitjans, M., 2015, Antitumor activities of metal oxide nanoparticles, *Nanomaterials*, 5 (2), 1004–1021.
- [14] Picatonotto, T., Vione, D., Carlotti, M.E., and Gallarate, M., 2001, Photocatalytic activity of inorganic sunscreens, *J. Dispersion Sci. Technol.*, 22 (4), 381–386.
- [15] Hoang, B.T., and Popa, I., 2014, Innovation in inorganic UV filters in sunscreen, *H&PC Today*, 9 (3), 35–39.
- [16] Goudarzi, A., Aval, G.M., Sahraei, R., and Ahmadpoor, H., 2008, Ammonia-free chemical bath deposition of nano crystalline ZnS thin film buffer layer for solar cells, *Thin Solid Films*, 516 (15), 4953–4957.
- [17] Lam, K.T., Hsiao, Y.J., Ji, L.W., Fang, T.H., Shih, W.S., and Lin, J.N., 2015, Characteristics of polymer-fullerene solar cells with ZnS nanoparticles, *Int. J. Electrochem. Sci.*, 10, 3914–3922.
- [18] Suhail, M.H., Abdullah, O.G., Ahmed, R.A., and Aziz, S.B., 2018, Photovoltaic properties of doped zinc sulfide/n-Si heterojunction thin films, *Int. J. Electrochem. Sci.*, 13, 1472–1483.
- [19] Bartolucci, A., 2015, Morphological characterization of ZnS thin films for photovoltaic applications, *Thesis*, University of Bologna, Italy.
- [20] Kalyanasundaram, S., Panneerselvam, K., and Kumar, V.S., 2013, Study on physical properties of ZnS thin films prepared by chemical bath deposition, *Asia Pac. J. Res.*, 1 (VIII), 5–14.
- [21] McCloy, J., and Tustison, R., 2013, *Chemical Vapor Deposited Zinc Sulfide*, 1st Ed., SPIE, USA.
- [22] Kaur, N., Kaur, S., Singh, J., and Rawat, M., 2016, A review on zinc sulphide nanoparticles: From Synthesis, properties to applications, *J Bioelectron. Nanotechnol.*, 1 (1), 5.
- [23] Mahammed, B.A., and Ahmed, L.M., 2017, Enhanced photocatalytic properties of pure and Cr-modified ZnS powders synthesized by precipitation method, *J. Geosci. Environ. Prot.*, 5 (10), 101–111.
- [24] Mohammed, B.A., and Ahmed, L.M., 2018, Improvement the photo-catalytic properties of ZnS nanoparticle with loaded manganese and chromium by co-precipitation method, *JGPT*, 10 (7), 129–138.
- [25] Greenwood, N.N., and Earnshaw, A., 1997, “Zinc, Cadmium and Mercury” in *Chemistry of the Elements*, 2nd Ed., Butterworth–Heinemann, Oxford, 1201–1220.
- [26] Gadalla, A., Abd El-Sadek, M.S., and Hamood, R., 2018, Synthesis, structural and optical characterization of Cds and ZnS quantum dots, *Chalcogenide Lett.*, 15 (5), 281–291.
- [27] Xu, X., Hu, L., Gao, N., Liu, S., Wageh, S., Al-Ghamdi, A.A., Alshahrie, A., and Fang, X., 2015, Controlled growth from ZnS nanoparticles to ZnS–CdS nanoparticle hybrids with enhanced photoactivity, *Adv. Funct. Mater.*, 25 (3), 445–454.
- [28] Raubach, C.W., de Santana, Y.V.B., Ferrer, M.M., Longo, V.M., Varela, J.A., Avansi, W., Buzolin, P.G.C., Sambrano, J.R., and Longo, E., 2012, Structural and optical approach of CdS@ZnS core-shell system, *Chem. Phys. Lett.*, 536, 96–99.
- [29] Madhavi, J., Basha, S.J., Khidhirbrahmendra, V., Rao, L.V.K., Reddy, C.V., and Ravikumar, R.V.S.S.N., 2017, Spectroscopic investigations on Mn²⁺ doped ZnS/CdS nanocomposite powder, *J. Chem. Pharm. Sci.*, 10 (1), 608–610.
- [30] Khezrianjoo, S., and Revanasiddappa, H.D., 2012, Langmuir-Hinshelwood kinetic expression for the photocatalytic degradation of metanil yellow aqueous solutions by ZnO catalyst, *Chem. Sci. J.*, 2012, CSJ-85.
- [31] Ahmed, L.M., 2018, Photo-decolorization kinetics of acid red 87 dye in ZnO suspension under different types of UV-A light, *Asian J. Chem.*, 30 (9), 2134–2140.
- [32] Abbas, N.K., Al-Rasoul, K.T., and Shanan, Z.J., 2013, New method of preparation ZnS nano size at low pH, *Int. J. Electrochem. Sci.*, 8, 3049–3056.
- [33] Nanda, J., Sapra, S., Sarma, D.D., Chandrasekharan, N., and Hodes, G., 2000, Size-selected zinc sulfide nanocrystallites: Synthesis, structure, and optical studies, *Chem. Mater.*, 12 (4), 1018–1024.

- [34] Shanan, Z.J., Al-Taay, H.F., Khaleel, N., Nader, R., Kaddum, E., and Talal, S., 2016, Structural and optical properties of chemically sprayed ZnS nanostructure, *IOSR-JAP*, 8 (5), 66–72.
- [35] Sarma, M.P., and Wary, G., 2015, Synthesis and optical properties of ZnS nanoparticles in PVA matrix, *Am. J. Mater. Sci. Technol.*, 4 (2), 58–71.
- [36] Anwar, H.A., and Jassem, S.A., 2015, Preparation and study of CdS thin films at different concentration thiourea by chemical bath deposition (CBD) method, *World Sci. News*, 23, 73–89.
- [37] Tyagi, C., Sharma, A., and Kurchania, R., 2014, Synthesis of CdS quantum dots using wet chemical co-precipitation method, *J. Non-Oxide Glasses*, 6 (2), 23–26.
- [38] Lee, H.L., Issam, A.M., Belmahi, M., Assouar, M.B., Rinnert, H., and Alnot, M., 2009, Synthesis and characterizations of bare CdS nanocrystals using chemical precipitation method for photoluminescence application, *J. Nanomater.*, 2009, 914501.
- [39] Yong, K.T., Sahoo Y., Swihart, M.T., and Prasad, P.N., 2007, Shape control of CdS nanocrystals in one-pot synthesis, *J. Phys. Chem. C*, 111 (6), 2447–2458.
- [40] Curti, E., 1997, Coprecipitation of radionuclides: Basic concepts, literature review and first applications, *PSI-97-08*, Switzerland.
- [41] Slav, A., 2011, Optical characterization of TiO₂-Ge nanocomposite films obtained by reactive magnetron sputtering, *Dig. J. Nanomater. Biostruct.*, 6 (3), 915–920.
- [42] Tauc, J., Grigorovici, R., and Vancu, A., 1966, Optical properties and electronic structure of amorphous Germanium, *Phys. Status Solidi B*, 15, 627–637.
- [43] Ahmed, L.M., Alkaim, A.F., Halbus, A.F., and Hussein, F.H., 2016, Photocatalytic hydrogen production from aqueous methanol solution over metalized TiO₂, *Int. J. ChemTech Res.*, 9 (10), 90–98.
- [44] McQuarrie, D.A., and Simon, J.D., 1997, *Physical Chemistry-A Molecular Approach*, 1st Ed., University Science Books, Sausalito, 11072.
- [45] Ahmed, L.M., Jassim, M.A., Mohammed, M.Q., and Hamza, D.T., 2018, Advanced oxidation processes for carmoisine (E122) dye in UVA/ZnO system: Influencing pH, temperature and oxidant agents on dye solution, *JGPT*, 10 (7), 248–254.
- [46] Ahmed, L.M., Tawfeeq, F.T., Abed Al-Ameer, M.H., Abed Al-Hussein, K., and Athaab, A.R., 2016, Photo-degradation of reactive yellow 14 dye (a textile dye) employing ZnO as photocatalyst, *J. Geosci. Environ. Prot.*, 4 (11), 34–44.
- [47] Ahmed, L.M., Abd-Kadium, E.Q., Salman, R.A., Wali, H.K., and Nasser, N.K., 2017, Photocatalytic decolorization of dispersive yellow 42 dye in ZnO/UV-A system, *Iraq. Nat. J. Chem.*, 17 (4), 199–209.